ESTIMATION OF SEDIMENT PROPERTIES USING AIR LAUNCHED SONOBUOYS

Subramaniam D Rajan
Scientific Solutions Inc.
453 Alberto Way
Los Gatos CA USA

1 INTRODUCTION

In shallow water, the ocean bottom plays a significant role in the propagation of acoustic energy. Hence, knowledge of the acoustic properties of the ocean bottom is critical in prediction of acoustic propagation in shallow water environments. The US Navy is developing a Multi-Static Active Coherent (MAC) acoustic search system that combines a newly developed coherent source sonobuoy with a field of receiver sonobuoys. With the availability of GPS (Global Positioning System) navigation in the sonobuoys, the feasibility of using data collected during Navy ASW operations to estimate sediment properties is now being explored. MOMAX (Modal Mapping Experiment) is an experiment in which the acoustic field from a moving coherent source on an array of freely drifting buoys equipped with hydrophones, GPS navigation, and radio telemetry are measured. One of the experiment goals is to estimate sediment properties from this data. This approach uses of modal eigenvalues for estimating the sediment properties and hence requires the acoustic field at the receiver to be a function of range which in the case of MOMAX experiments is achieved by a ship towing a source[1]. However, in the conceptual design of the MOMAX experiments, the source is carried by a sonobuoy. In such a situation, it is unlikely that the sonobuoy with the source will move out in range in relation to the receiver sonobuoys and create a horizontal array of sufficient aperture to extract the modal eigenvalues from the data.

A more realistic approach is to transmit a broadband signal from the source. The experimental set up in this case consists of a source carried by a sonobuoy that transmits broadband signals and several freely drifting receiver sonobuoys . Then the signals acquired by the network of receiver sonobuoys are processed to estimate the mode dispersion data. This forms the data set used to obtain the acoustic properties of the sediments[2]. Typically, one assumes that the water column properties are known by direct measurement and the only unknowns to be estimated are the acoustic characteristics of the bottom.

In order to extract the mode dispersion data from the signal acquired at the receiver a time frequency analysis is done using Short Time Fourier Transform (STFT). The squared modulus of the STFT is the spectrogram. This procedure provides the travel time for each mode to travel from source to receiver as a function of frequency. If the distance from the source to receiver is short, the modes are not fully developed and the STFT procedure does not yield the mode dispersion data. In such cases time warping procedure[3] can be used to extract mode dispersion information. Another advantage of the warping method is that the mode dispersion data can also be extracted for weak modes, when it is not possible with STFT.

In the following sections, we present results of a simulation study in which we have simulated a distributed network of sonobuoys with a source carrying sonobuoy located in the middle. The sonobouys in the different regions have different water column depths and different bottom properties. We explore the ability of the inverse algorithm to extract sediment properties in the different areas.

2 SIMULATION STUDY

2.1 Simulation of environment

The estimation of sediment properties in shallow water areas is difficult because of the bathymetry in these areas are complex giving rise to varying water column depths as well as varying sediment characteristics. In order to represent such an environment an area off the coast of New Jersey for which the bathymetry is known was used in this simulation. Figure 1 show the region that was used in creating the data for this simulation together with the locations of 25 sonobuoys and the source. The locations of the sonobuoys were obtained assuming that they were uniformly distributed over the defined limits of the region as indicated by their Longitudes and Latitudes. The area covered by the sonobuoys was then divided in to six regions as shown in Figure 1

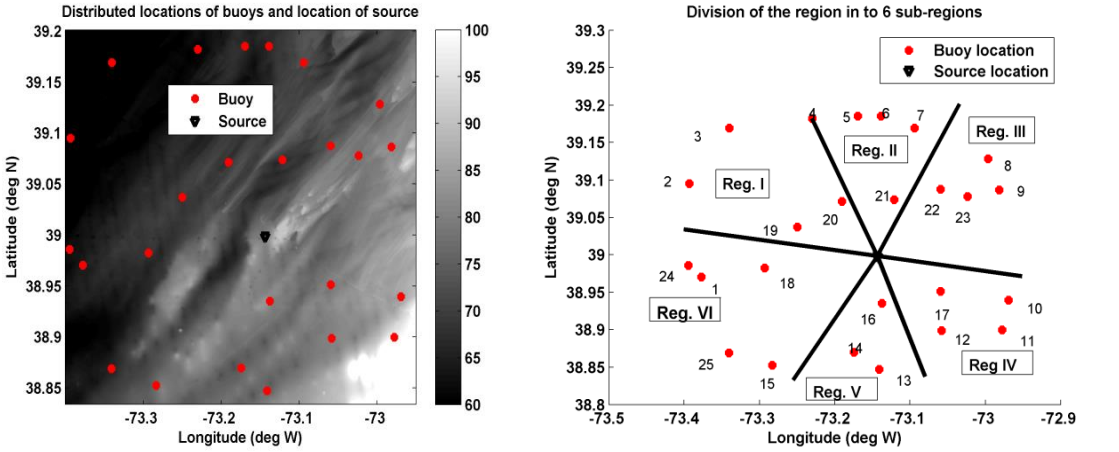

Figure 1; The panel on the left shows the location of the distributed network of sonobuoys and the location of the source The figure also shows bathymetry of the area which varies from 60 m to 100 m. The right panel shows the six major regions in to which the area has been sub-divided.

Because of the differences in the water column depths along the different source/buoy transects we made assumptions that the sediment properties also varied along these different sections. In regions where there was a large variation in water column depths we assumed the the bottom properties were different. For example in the area where buoys 2,3 19 and 20 are located there are three distinct depth regions namely region of an average depth of 72 m followed by a region of an average depth of 69 m and then the final section with an average depth of 60 m. In this case we assumed that the regions where the depth are 72 m and 69 m the bottom properties are identical where as the region where the depth changed to 60 m has a different bottom properties. Similarly by looking at the depth variations in the different parts we created a total of seven regions with slightly different sediment properties. In each of these sections different bottom models were assumed and these are termed model M1 to M7 as shown in Figure 2. The number of sediment layers and their thicknesses have also been varied and are similar to sediment layering found in the area in earlier experiments[1]. The details of the compressional wave speed profiles for the seven bottom models are shown in Figure 2. In all cases the terminating half space is assumed to have a compressional wave speed of 1850 m/s. The sediment density values were set at 1.6 gm/cc in all the layers and in the terminating half space. Attenuation in the sediment layers and terminating halfspace have been neglected. The sound speed structure in the water column was assumed to be the same over the entire area.

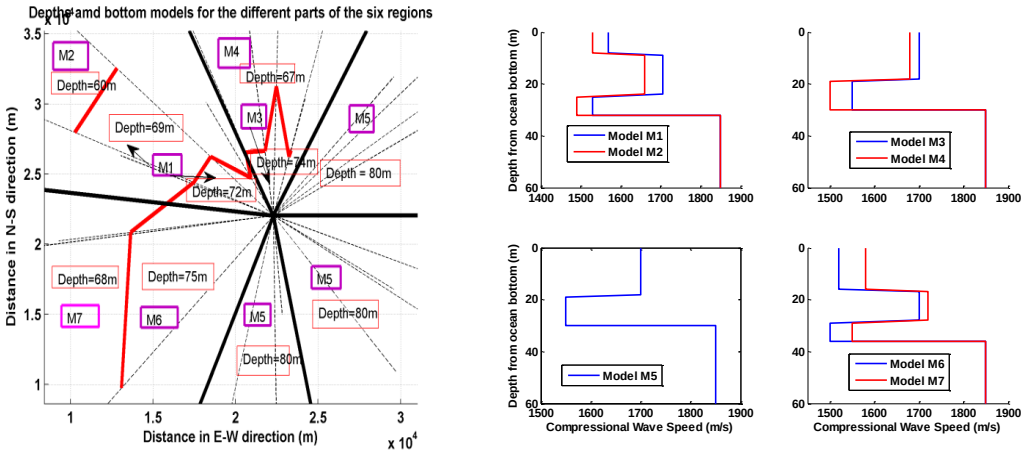

Figure 2. The left panel of the figure shows the six major divisions of the region together with the variations in the depths within these regions. It also indicates the seven bottom models used to describe the range dependent sediment properties. The compressional wave speed profiles of the seven bottom models are shown in the right panel of the figure.

2.2 Broad Band Signal Generation

Broadband signals that have found wide acceptance are the LFM (Linear Frequency Modulated) signals or chirps in which the frequency is varied linearly either going up or down with the signal duration. Broadband signals are also created using pseudorandom sequences[4]. The sequence of zeros and ones generated by the sequence is used to modulate a carrier signal. For creating the transmitted signal the zeros in the sequence is changed to -1, (i.e. we now have a sequence of 1 and -1). Each digit in the sequence is a chip. If the sequence has N digits, the signal has N chips. The length of each chip defines the bandwidth of the signal. The numbers of cycles of the carrier signal that form a chip determines the bandwidth of the signal.

2.3 Computation of Signals Acquired by the Sonobuoys.

In order to compute the signal acquired by the buoys the distances from the source to the receiver are required. These are obtained from the known positions of the source and the respective buoys. A time-domain acoustic signal at the receiver is obtained by Fourier synthesis of the frequency domain solution to the acoustic wave equation using the expression below.

$$p(r,z,t) = \int_{-\infty}^{\infty} S(\omega) p(r,z,\omega) \exp(i\omega t)\, d\omega \qquad (1)$$

where $S(\omega)$ is the spectrum of the transmitted signal and $p(r,z,\omega)$ is the frequency domain solution at range *r* and depth z. To compute the time domain solution above requires that $p(r,z;\omega)$ be calculated at a number of discrete frequencies, which span the frequency band of the source spectrum. The ocean environment was the input to the normal mode code KRAKEN[5] for computing the frequency domain solution with the range to the receiver, depths of the source, and receiver set as required.

The signal acquired by the receiver is a convolution of the impulse response of the channel with the transmitted pulse. Before processing the signal acquired by the buoys, it is necessary to extract the impulse response of the channel, to take out the time-frequency variation of the transmitted signal during signal duration. This is done by de-convolution of the received signal. In the simulation study presented here, the deconvolution of the signal is done in the frequency domain. The impulse response is then used to perform the time-frequency analysis using STFT or warping procedure.

2.4 Inversion for Compressional Wave Speed Profiles

The inversion for the sediment compressionalwave speed profiles for the seven areas as represented in models M1 to M7 was performed using the mode dispersion data obtained from the signals recived at the buoys. All inversions were carried out for the compressional wave speed in the layers. All other parameters namely the compressional wave speedin the terminating half space and the density value of the sediment layers and the terminating half space were assumed to be known.

Consider the bottom model M2. In this case, the water column has a depth of 60 m. The sediment has three layers of thickness 8 m, 16 m and 8m.The compressional wave speed in the layers are 1530 m/s, 1660 m/s and 1490 m/s respectively. The terminating half space has value of 1850 m/s. The density in the sediment layers and the terminating half space is 1.6 gm/cc. Examination of the mode function indicates that in order to estimate the bottom model correctly we need to know the mode travel time at frequencies including those that are below the Airy phase. In many cases, the strength of the modes at frequencies below the Airy phase is very low and therefor it is difficult to estimate the mode travel time at these frequencies..

In order to estimate the values of the mode travel time at frequencies below the Airy phase the bottom model was first estimated using the mode dispersion data at frequencies above Airy phase. Using the bottom model thus obtained mode dispersion was computed theoretically to get approximate mode travel times at frequencies below the Airy phase. This was then incorporated in the input data. Using this approach repeatedly, the estimates of mode arrivals at frequencies below the Airy phase were incrementally improved and the more correct estimates of the bottom compressional wave speed profiles were obtained.

Another issue that needs attention is determination of the number of sediment layers and their thickness. If the number of layers and their thicknesses are known then they are input to the inversion process. The inversion involves obtaining the inverse of a matrix as described in[2]. This matrix is generally ill conditioned and need some form of regularization. We have used qualitative regularization[6,7] in obtaining the inverse solution and this requires data on sediment layering as input to the inversion. In order to have an estimate of the number of layers and their thicknesses we performed inversion without any layer data i.e. without incorporating qualitative regularization. The result of inversion in the region of model M2 is shown in Figure 3. This indicates that the compressional wave speed in the sediment has a low speed top layer which is followed by a high speed layer and a low speed layer again. The high speed layer in the middle has a thickness about twice as that of the low speed layers. This led us to assume a bottom model comprising of three layers of depths 8 m, 16 m and 8m respectively.

In the analysis of data in the frequency range 250 Hz – 310 Hz there was a problem that was resolved by re-assigning the mode number. Let us consider the model M5. The bottom model is a two-layer one with top layer of thickness 18 m and a second layer of thickness 12 m. This is followed by a terminating half space. The compressional wave speed in the top layer is 1700 m/s and in the bottom layer it is 1550 /s. In the terminating half space, the compressional wave speed is 1850 m/s. The density is 1.6 gm/cc in the sediment layers and in the half space. The top left panel of Figure 4 shows the spectrogram obtained by performing STFT of the signal at the receiver, which in this case is located at a distance of 19270 m from the source. The spectrogram shows that the mode dispersion curves for all the modes vary smoothly from its value at 250 Hz to its value at 500 Hz. Theoretical mode dispersion curves for modes 11, 12 and 13 obtained using the known water column and sediment properties are overlaid on the spectrogram in Figure 4. The mode dispersion curves obtained from theory for the true ocean and bottom model show that there are jumps in the mode dispersion curves. Further part of the dispersion curve aligns with a lower mode as displayed in the spectrogram. This happens for certain modes that are resonant...

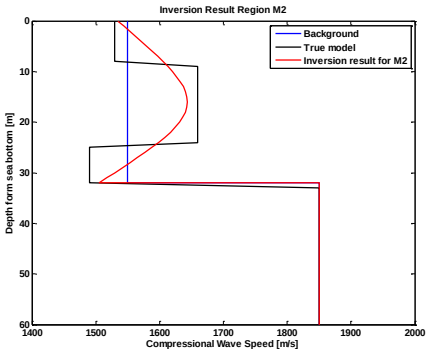

Figure 3: Inversion for rmodel M2 without discontinuity incorporated in inversion procedure(Redline). The blackline is the true model and the blue line is the starting model.

It is seen from the plots in the top left panel of Figure 4 that part of mode 13 as per theory is aligned with mode 12 in the spectrogram. Similar features occur in the case of other modes above mode 10. The incorrect identification of modes due to this anomaly will lead to large errors in inverse results. In the top right panel of Figure 4, we plot the group speed of modes 1 to 16 at 250 Hz. These are represented in black dots. We notice that two values i.e. those for mode 11 and 15 are much higher than the rest. These are the modes where the resonance is observed. We now re-assign the mode number of the modes eliminating the resonant modes. We now have 14 modes instead of 16. What was originally mode 12 has now become mode 11 and so on. This is shown as red circle in the figure. We do this for modes at each frequency and with this; a modified mode dispersion data is obtained. In the bottom panel of Figure 4, we plot the modified mode dispersion data on the spectrogram. It is seen that the curves follow the modes as displayed in the spectrogram. In adopting this procedure, we identified resonant modes i.e. by identifying sharp increases in the group speed and eliminated those modes. Simultaneously we made suitable changes to the mode function and eigenvalues associated with the modes.

The results of the inversion performed using data in the frequecy range 50 Hz – 110 Hz and in the range 250Hz – 310Hz are shown in Figures 5 for four of the seven regions. It is seen from the results that the bottom model that was obtained using data at the lower frequencies are closer to the true bottom model when compared to the results using data from the higher frequencies.This is to be expected as mode function at the higher frequecies decay fast with sediment depth and hence the larger errors while using data from higher frequencies. There are also larger errors while performing range-dependent inversions. Bottom models for the remaining three regions also show similar trends in the results.

2.5 Validation of Results

The differences between the true bottom models and the models obtained by inversion of the mode dispersion data are evident in Figure 5. We now investigate how these differences in bottom model affect acoustic fields predicted by these sediment models even though the differences from the true model are small. We study this at three frequencies 50 Hz, 250 Hz and 500 Hz. In performing this computation we considered the transmission from the source to the receiver at the location of sonobuoy 2. In Figure 6 the fields as predicted by the inverted bottom models are compared with the field as predicted by the true bottom model.

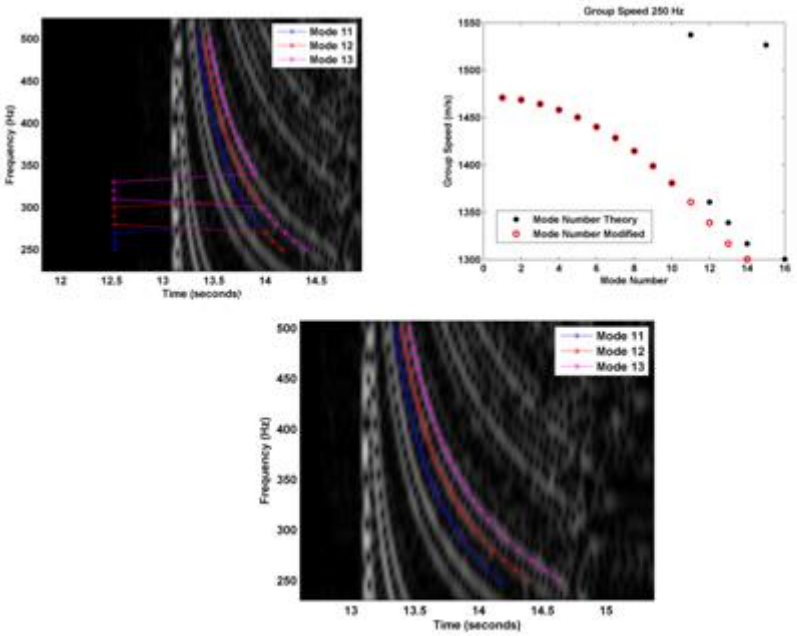

Figure 4: The top left panel shows the spectrogram with the theoretical dispersion curves for modes 11,12 and 13 overlaid. In the top right panel we have plotted (black spots) the group speed for the first 16 modes at 250 Hz. Overlaid are the group speed after deleting those which are outliers (red circle). The bottom panel shows the revised dispersion curves obtained after deleting the outliers over laid on the spectrogram.

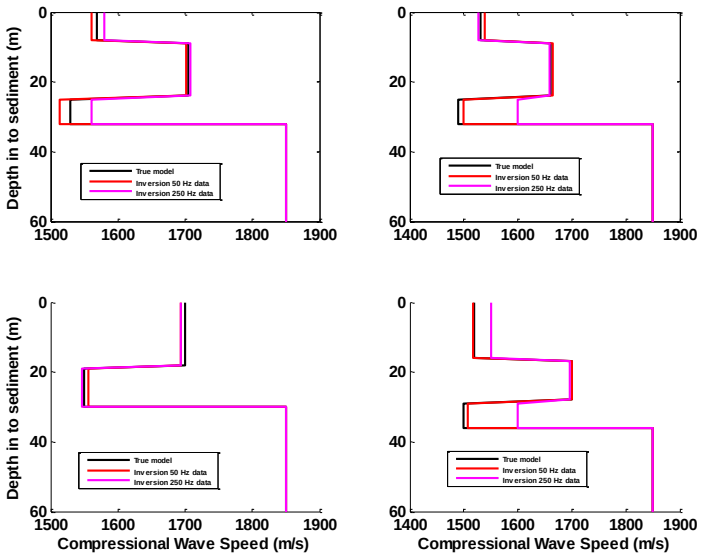

Figure 5: True bottom model and the inverted model for bottom models. The top panels shows the result for M1 and M2. The bottom panels show the results for M3 and M6. In the plots the true bottom mdoels (Black) are compared with models obtained from data in the frequency range 50Hz -110Hz(Red) and models obtained from data in the frequency range 250Hz – 310 Hz((Magenta).

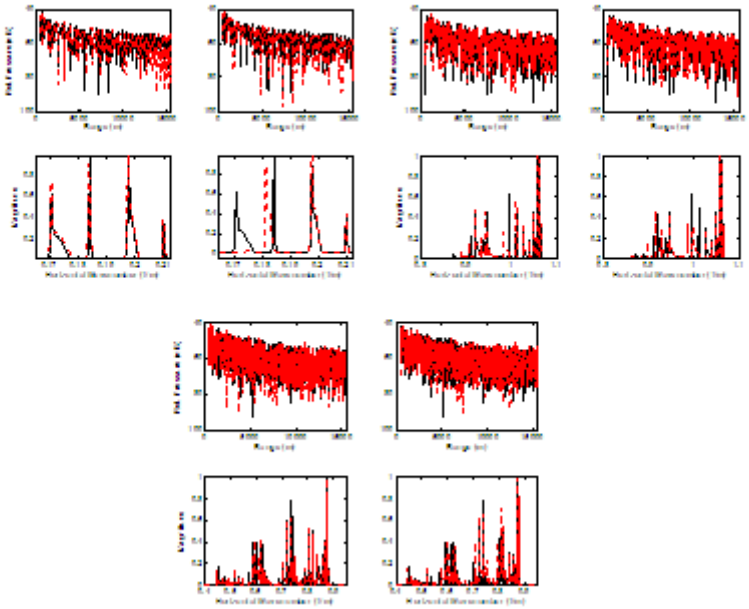

Figure 6: The row 1 of the plots are the field at 50 Hz predicted by models obtained from 50 Hz -110 Hz data followed by field predicted using model from 250 Hz- 310 Hz data. This is followed by fields at 250 Hz predicted using models from 50 Hz – 110Hz data and 250 Hz -310 Hz data. Beneath each of the fields are the plots of the wave number spectrum associated with these fields. In row 3 the fields at 500 Hz as predicted by bottom models from 50 Hz -110 Hzdata and 250 Hz -310 Hz data are shown. Beneath the fieds are the corresponding wave number spectrum.In all plots the black lines are the predictions by the true bottom model and the dotted red lines are the fields predicted by the inverted botom model.

The field at 50 Hz as predicted by model from 50 Hz -110 Hz data is in good agreement with the field predicted by the true bottom model up to 5000 m after which the differences increases with range. The wave number spectrum for the true field and the field predicted by the model are in very close agreement except in the case of modes 3 and 4. This shows how even small differences in the wavenumber spectrum cause differences in the field which accumulate with range. In the case of field obtained using the bottom model from 250 Hz – 310 Hz data the fields the agreement between the fields are not as good as in the previous case. It is seen form the wave number spectrum that mode 4 in very weak. Further there is a large error in the wavenumber of mode 3 between that of the true field and the field from the inverted model. These differences in the wavenumber spectrum contribute to the differences between the fields. In the case of predictions at 250 Hz the predicted field generally follows the true field in terms oftheir magnitudes though there are differences in the interference pattern. The wave nuber spectrum of the fields show marked differences in the spectrum which results in the differences in the interference patterns. The same is true in the case of field predicted at 500 Hz.

Table 1. Correlation values between true field and field predicted by inverted models.

Frequency (Hz)	Model using 50 Hz – 110 Hz data	Model using 250 Hz – 310 Hz data
50	0.8835	0.8805
250	0.9040	0.8914
500	0.8361	0.8329

To quantify these differences the correlation value between the true field and the field predicted by the inverted bottom models are presented in Table 1. The correlation values were obtained using the field magnitudes over a range of 15,000 m.

3. CONCLUSIONS

The purpose of the study described in the paper is to investigate whether routine Naval operations can be suitably modified to collect data that can be used to estimate sediment properties. Such a capability will provide critical inputs to sonar performance evaluation while operating in shallow water areas. The methodology used for estimating range-dependent and range independent sediment properties have been well documented in the literature[2]. The task was therefore to see how these well known method will perform in an environment which has complicated range-dependent sediment structure and at different frequency ranges. A suitable environment was created using the well surveyed area off the coast of New Jersy. The different regions of this environment have differing depths and varying sediment properties were assumed for these regions. The inversions were carried out at two frequency ranges i.e. 50 Hz – 110 Hz and 250 Hz – 310 Hz using methodologies developed for range independent and range-dependent inversions.The results of inversions show that it is possible to extract the sediment properties though the errors are more when range-dependent inversions are involved. The evaluation of the inverted bottom models indicate that the models can predict fields at 50 Hz, 250 Hz and 500 Hz but with errors that increase with range as expected. Further work using data from higher frequencies namely 500 Hz, 1000 Hz and above is in progress.

4 REFERENCES

1. G. V. Frisk. K. M. Becker, S. D. Rajan, C. J. Sellers, Keith von der Heydt, C. M. Smith, and M. S. Ballard, ”Modal Mapping Experiment and geoacoustic iinversion using sonobuoys,” IEEE J. Ocean. Eng.,40, No.3 ,607-620,2015.

2. S. D. Rajan, G. V. Frisk, K. M. Becker, J. F. Lynch, G. Potty, and J. H. Miller, “Modal inverse techniques for inferring geoacoustic properties in shallow water,” in Important Elements in: *Geoacoustic Inversion, Signal Processing, and Reverberation in Underwater Acoustics 2008*, A. Tolstoy, Ed. Kerala, India: Research Signpost, 2008, pp. 165–234.
3. J. Bonnel, B. Nicholas, J. Mars and S. C. Walker, ”Estimation of modal group velocities with a single receiver for geoacoustic inversion in shallow water, “Journal of the Acoustical Society of America, 128,719-727,2010
4. *Spread spectrum systems with commercial applications*, R. C. Dixon, John Wiley & Sons, 1994.
5. M. Porter, The Kraken Normal Mode Program, Saclant Under Sea Research Center, La Spezia, Italy, Tech Report SM245, 1991.
6. L. Simcik and P. Lin,” Qualitative regularization: Resolving non-smooth solutions. Tech Report CSE 94-12, University of California, Department of Mathematics.
7. M. S. Ballard, K. M. Becker, and J. A. Goff, “Geoacoustic Inversion for the New Jersey shelf: Three dimensional sediment model,” IEEE J. Ocean. Eng., vol. 35, no. 1, pp. 28–42, Jan. 2010.